HHS Public Access

Author manuscript

Hepatology. Author manuscript; available in PMC 2023 February 21.

Published in final edited form as:

Hepatology. 2021 October ; 74(4): 1932–1951. doi:10.1002/hep.31864.

Myelocytomatosis-Protein Arginine N-Methyltransferase 5 Axis Defines the Tumorigenesis and Immune Response in Hepatocellular Carcinoma

Yuhong Luo[1,*], **Yuqing Gao**[2,3,*], **Weiwei Liu**[4,*], **Yuan Yang**[5], **Jie Jiang**[6], **Ying Wang**[2], **Wei Tang**[7], **Shoumei Yang**[1], **Lulu Sun**[1], **Jie Cai**[1], **Xiaozhen Guo**[2], **Shogo Takahashi**[1,8], **Kristopher W. Krausz**[1], **Aijuan Qu**[9,10], **Lei Chen**[5,11], **Cen Xie**[1,2,6], **Frank J. Gonzalez**[1]

[1]Laboratory of Metabolism, Center for Cancer Research, National Cancer Institute, National Institutes of Health, Bethesda, MD, USA

[2]State Key Laboratory of Drug Research, Shanghai Institute of Materia Medica, Chinese Academy of Sciences, Shanghai, P.R. China

[3]University of Chinese Academy of Sciences, Beijing, P.R. China

[4]Department of Laboratory Medicine and Central Laboratory, Shanghai Tenth People's Hospital, Tongji University, Shanghai, P.R. China

[5]Eastern Hepatobiliary Surgery Hospital, Second Military Medical University, Shanghai, P.R. China

[6]School of Chinese Materia Medica, Nanjing University of Chinese Medicine, Nanjing, P.R. China

[7]Molecular Epidemiology Section, Laboratory of Human Carcinogenesis, Center for Cancer Research, National Cancer Institute, National Institutes of Health, Bethesda, MD, USA

[8]Department of Biochemistry and Molecular & Cellular Biology, Georgetown University, Washington, DC, USA

[9]Department of Physiology and Pathophysiology, School of Basic Medical Sciences, Capital Medical University, Beijing, P.R. China

[10]Key Laboratory of Remodeling-Related Cardiovascular Diseases, Ministry of Education, Beijing, P.R. China

ADDRESS CORRESPONDENCE AND REPRINT REQUESTS TO: Lei Chen, Ph.D., International Co-operation Laboratory on Signal Transduction, Eastern Hepatobiliary Surgery Institute, Second Military Medical University, 255 Changhai Road, Shanghai 200438, P.R. China, chenlei@smmu.edu.cn, Tel.: +1-86-21-81875361, Cen Xie, Ph.D., State Key Laboratory of Drug Research, Shanghai Institute of Materia Medica, Chinese Academy of Sciences, 501 Haike Road, Shanghai 201203, P.R. China, xiecen@simm.ac.cn, Tel.: +1-86-21-20231965, Frank J. Gonzalez, Ph.D., Laboratory of Metabolism, Center for Cancer Research, National Cancer Institute, Bethesda, MD 20892, gonzalef@mail.nih.gov, Tel.: +1-240-760-6875.

*These authors contributed equally to this work.

Author Contributions: Y.L., Y.G., J.J., Y.W., S.Y., L.S., J.C., and C.X. performed the experiments. W.L. and Y.Y. collected the urine samples and biopsies from patients with HCC and healthy humans. W.T. analyzed the RNA-seq data. S.T. helped with ChIP assay.K.W.K. and X.G. helped with the metabolomics analysis. Y.L., Y.G., A.Q., L.C., C.X., and F.J.G. were responsible for the study concept and design. Y.L., Y.G., C.X., and F.J.G. wrote the manuscript. L.C., C.X., and F.J.G. supervised the study.

Potential conflict of interest: Nothing to report.

Supporting Information

Additional Supporting Information may be found at onlinelibrary.wiley.com/doi/10.1002/hep.31864/suppinfo.

[11]International Co-operation Laboratory on Signal Transduction, Eastern Hepatobiliary Surgery Institute, Second Military Medical University, Shanghai, P.R. China

Abstract

BACKGROUND AND AIMS: HCC is a leading cause of cancer-related deaths globally with poor outcome and limited therapeutic options. Although the myelocytomatosis (*MYC*) oncogene is frequently dysregulated in HCC, it is thought to be undruggable. Thus, the current study aimed to identify the critical downstream metabolic network of MYC and develop therapies for MYC-driven HCC.

APPROACH AND RESULTS: Liver cancer was induced in mice with hepatocyte-specific disruption of *Myc* and control mice by administration of diethylnitrosamine. Liquid chromatography coupled with mass spectrometry-based metabolomic analyses revealed that urinary dimethylarginine, especially symmetric dimethylarginine (SDMA), was increased in the HCC mouse model in an MYC-dependent manner. Analyses of human samples demonstrated a similar induction of SDMA in the urines from patients with HCC. Mechanistically, *Prmt5*, encoding protein arginine N-methyltransferase 5, which catalyzes SDMA formation from arginine, was highly induced in HCC and identified as a direct MYC target gene. Moreover, GSK3326595, a PRMT5 inhibitor, suppressed the growth of liver tumors in human MYC-overexpressing transgenic mice that spontaneously develop HCC. Inhibition of PRMT5 exhibited antiproliferative activity through up-regulation of the tumor suppressor gene *Cdkn1b/p27*, encoding cyclin-dependent kinase inhibitor 1B. In addition, GSK3326595 induced lymphocyte infiltration and major histocompatibility complex class II expression, which might contribute to the enhanced antitumor immune response. Combination of GSK3326595 with anti–programed cell death protein 1 (PD-1) immune checkpoint therapy (ICT) improved therapeutic efficacy in HCC.

CONCLUSIONS: This study reveals that PRMT5 is an epigenetic executer of MYC, leading to repression of the transcriptional regulation of downstream genes that promote hepatocellular carcinogenesis, highlights a mechanism-based therapeutic strategy for MYC-driven HCC by PRMT5 inhibition through synergistically suppressed proliferation and enhanced antitumor immunity, and finally provides an opportunity to mitigate the resistance of “immune-cold” tumor to ICT. (HEPATOLOGY 2021;74:1932–1951).

Liver cancer is the third leading cause of cancer-related deaths worldwide and is very aggressive, with a low 5-year survival rate of 20%.[(1)] HCC is the most common liver cancer, representing up to 75% of all primary hepatic malignancies. Current first-line treatment for HCC is limited to the kinase inhibitors sorafenib, regorafenib, and lenvatinib, but resistance is a matter of course.[(2)] Thus, it is necessary to further understand the molecular pathogenesis of HCC to identify drug targets for its treatment.

Myelocytomatosis (MYC) is a highly pleiotropic transcription factor that modulates many genes involved in a variety of biological processes like cell proliferation, metabolism, apoptosis, adhesion, and differentiation.[(3)] Dysregulation of MYC is commonly found in various human cancers including HCC and is frequently associated with poor prognosis and survival.[(4)] In rodent models, the human-derived MYC transgene spontaneously prompted HCC development, and hepatocyte-specific MYC disruption suppressed HCC

tumorigenesis.[5,6] Functional analysis of HCC gene expression profiles revealed that MYC plays a central role during malignant conversion in tumorigenesis.[7] Hence, therapeutic strategies aimed at inhibiting MYC expression or activity would be a promising route to treat liver cancer. However, to date, there is no therapy directly disrupting MYC function owing to its "undruggable" protein structure. Identifying critical genes downstream of MYC can help develop alternative strategies for the treatment of MYC-driven HCC.

Transcriptional activation by MYC occurs through dimerization with its partner protein max (MAX) and direct binding to a 6-nucleotide DNA consensus sequence CACGTG, designated the E-box. In contrast to transcriptional activation, the mechanisms by which MYC silences gene expression remain to be elucidated. The causes of HCC are heterogeneous, with both genetic and epigenetic alterations associated with tumor progression. Accumulating evidence has revealed the relevance of aberrant epigenetic modifications in HCC progression.[8] Genes affected by epigenetic alterations in HCC are highly overlapping with the MYC regulation network.[9] Thus, it is reasonable to assume that MYC may indirectly influence downstream metabolic events through epigenetic regulation.

Here, MYC-dependent alterations in the metabolome associated with HCC were explored by use of temporal hepatic-specific *Myc* disrupted mice ($Myc^{\Delta Hep,ERT2}$). Urinary dimethylarginine (DMA), especially symmetric DMA (SDMA), was found increased in HCC in an MYC-dependent manner. Protein arginine N-methyltransferase (*Prmt*) 5, encoding the predominant type II arginine methyltransferase responsible for the symmetric dimethylation of arginine residues, was identified as a direct MYC target gene. These data suggested that MYC drives transcription at least partially through regulating PRMT5 in HCC, and targeting PRMT5 might be an alternative therapeutic approach for MYC-driven HCC. Several studies reported the role of PRMT5 in HCC,[10,11] supporting the rationale for PRMT5 inhibition in HCC treatment. However, most of these studies used HCC cell lines or xenograft models and only focused on the regulation of cancer cells by PRMT5 without considering the immunogenic features in HCC. HCC is more heterogeneous than other types of solid cancer and hematological malignancies and is not associated with a specific driver mutation. Compelling evidence indicates that the immune system strongly influences HCC development.[12–14] Thus, combinatory use of immunotherapy with a molecular targeted agent has advanced rapidly in recent years. Notably, the current study demonstrated that inhibition of PRMT5 by GSK3326595 suppressed MYC-driven liver tumor growth in human MYC-transgenic mice that spontaneously develop HCC through both suppressed proliferation through up-regulation of p^{27} and enhanced antitumor immunity through induction of lymphocyte infiltration and major histocompatibility complex class II (MHC II) expression. The combination therapy of PRMT5 inhibitor and anti–programmed cell death protein 1 (PD-1) antibody showed superior antitumor response compared with each therapy alone. These findings show the functional importance of the MYC-PRMT5 axis during liver tumorigenesis and provide a rationale for therapeutic option of MYC-driven HCC through PRMT5 inhibition from both tumorigenic and immunogenic aspects.

Patients and Methods

HUMAN COHORTS

Urine samples, paired liver tumors, and adjacent nontumor tissues were taken from three respective cohorts. Urine samples were collected from a cohort of 372 participants (196 patients with HCC and 176 healthy controls) and a cohort of 19 patients with HCC. Paired liver tumor and adjacent nontumor tissues were collected from a cohort of 43 patients with HCC and a cohort of 19 patients with HCC. Clinical information for these three cohorts is summarized in Supporting Table S1. The study protocol conformed to the ethical guidelines of the 1975 Declaration of Helsinki was priori approved by the Research Ethics Committee of Eastern Hepatobiliary Surgery Hospital and the Research Ethics Committee of Shanghai Tenth People's Hospital, and written informed consent was obtained from all individuals before participation in the study.

MOUSE STUDIES

Myc$^{fl/fl}$ mice were described.[5] The tetracycline operator (tetO)-MYC transgenic mice and tetracycline-controlled transactivator protein (tTA) transgenic mice were obtained from Dr. Tim F. Greten (National Cancer Institute, Bethesda, MD).[15] See the Supporting Information and Fig. S1 for schematic diagrams of the mouse studies. Mice were maintained under a standard 12-hour light/12-hour dark cycle with water and food provided *ad libitum*. All mouse studies were approved by the National Cancer Institute Animal Care and Use Committee and all animals received humane care according to the criteria outlined in the NIH Guide for the Care and Use of Laboratory Animals.

Results

URINARY METABOLIC SIGNATURE IS MYC-DEPENDENTLY ALTERED IN HCC

Consistent with published work,[5] 100% of the *Myc*$^{fl/fl}$ mice, although less than half of the *Myc*$^{\Delta Hep,ERT2}$ mice, developed liver tumors, demonstrating that hepatocyte-specific *Myc* disruption decreased HCC development (Fig. 1A; Supporting Table S2). A urinary metabolomic approach was engaged to provide important clues to study the mechanism of liver tumorigenesis. Partial least squares discriminant analysis distinguished different metabolic profiles between diethylnitrosamine (DEN)-treated *Myc*$^{fl/fl}$ and *Myc*$^{\Delta Hep,ERT2}$ mice (Fig. 1B). Compared with *Myc*$^{fl/fl}$ mice, a total of 136 metabolite features were significantly decreased and 12 features were significantly increased in *Myc*$^{\Delta Hep,ERT2}$ mice (Fig. 1C). Kyoto Encyclopedia of Genes and Genomes (KEGG) pathway analysis further showed that ablation of MYC in the liver mainly influenced amino acid and nucleic acid biosynthesis and metabolism, coincident with the decreased HCC tumorigenesis in *Myc*$^{\Delta Hep,ERT2}$ mice (Fig. 1C). Interestingly, the variable importance in projection score of the identified metabolites ($P < 0.05$) indicated that the histone methylation-related metabolite DMA was among the top differential metabolites that resulted in the group separation (Fig. 1C). There are two types of arginine dimethylation: SDMA and asymmetric DMA (ADMA). Only SDMA was significantly increased in HCC-prone DEN-treated *Myc*$^{fl/fl}$ mice compared with saline-treated *Myc*$^{fl/fl}$ mice, whereas the induction was depleted in *Myc*$^{\Delta Hep,ERT2}$ mice (Fig. 1D). Furthermore, the DEN-treated *Myc*$^{\Delta Hep,ERT2}$

mice had lower SDMA levels as early as 1 month after DEN injection, although there were no tumors at this timepoint, suggesting SDMA associated to a danger signal and a causative factor for HCC (Fig. 1E). Similar to the mouse data, the levels of SDMA, not ADMA, were increased in urine samples from patients with HCC compared with healthy controls and positively correlated with serum alpha-fetoprotein (Fig. 1F). These findings suggest that protein arginine methylation status is altered by MYC activation during HCC carcinogenesis.

MYC INDUCES PRMT5 EXPRESSION IN HCC

Next, the expression of protein arginine methyltransferases was determined. Among the genes examined, the level of *Prmt5* mRNA, encoding the predominant type II arginine methyltransferase responsible for the symmetric dimethylation of arginine residues, was higher in liver tumors compared with adjacent nontumor tissues in $Myc^{fl/fl}$ mice. By contrast, decreased *Prmt5* mRNA expression was observed after hepatic ablation of *Myc* (Fig. 2A). The levels of PRMT5 protein and its two products, H3R8me2s and H4R3me2s, were decreased in the livers of DEN-treated $Myc^{\Delta Hep,ERT2}$ mice compared with similarly treated $Myc^{fl/fl}$ mice (Fig. 2B). Consistent with the mouse data, human HCC had increased levels of MYC, PRMT5, H4R3me2s, and H3R8me2s proteins compared with adjacent nontumor tissues (Fig. 2B,C; Supporting Fig. S2A,B), paralleled by increased *MYC* and *PRMT5* mRNA expression (Fig. 2C; Supporting Fig. S2C). *PRMT5* mRNA levels in human liver tumors were positively correlated with the *MYC* mRNA levels (Fig. 2C; Supporting Fig. S2D). Similar results were observed at the protein levels (Supporting Fig. S2E). Bioinformatic analysis of three liver cancer datasets (Oncomine) also revealed increased expression of *PRMT5* in human liver tumors (Supporting Fig. S2F-H). These data indicate that MYC-induced HCC carcinogenesis is associated with changes in PRMT5-mediated epigenetic modifications. Furthermore, MYC, PRMT5, H4R3me2s, and H3R8me2s protein levels in human liver tumors were positively correlated with the urinary SDMA levels (Supporting Fig. S2I), supporting the view that up-regulation of urine SDMA results from MYC-PRMT5 overexpression in liver tumors.

To further dissect the mechanistic basis of PRMT5 dependency in MYC-driven HCC, MYC expression and activity were manipulated in different liver tumor cell lines. MYC overexpression increased, whereas inhibition of MYC by 10058-F4, which disrupts the MYC/MAX dimerization and prevents the transactivation of MYC target genes, decreased *PRMT5* mRNA and PRMT5 protein expression (Fig. 2D; Supporting Fig. S2J), suggesting that *PRMT5* might be a target of MYC. To determine whether MYC directly regulates *PRMT5* transcription, six putative E-boxes were found within 3 kb upstream and 1 kb downstream of the *PRMT5* transcription start site. (Blocks A-D) containing the predicted E-boxes were cloned into the pGL4.11 reporter vectors and luciferase reporter gene assays performed. In HepG2 cells transfected with pGL4.11-PRMT5 A-D, overexpression of MYC significantly induced A/C/D luciferase activity except B reporter (Fig. 2E). Chromatin immunoprecipitation (ChIP) assays were then carried out on cross-linked soluble chromatin isolated from the livers of MYC transgene turned on (MYC-ON) mice and MYC transgene turned off (MYC-OFF) mice. MYC recruitment to the *Prmt5* promoter was induced by MYC transgene overexpression. *Ccnd2*, encoding cyclin D2, which is a bona fide MYC

target gene, served as a positive control (Fig. 2F). Together, these results support the notion that MYC directly activates *PRMT5* transcription in HCC.

INHIBITION OF PRMT5 SUPPRESSES MYC-DRIVEN HCC DEVELOPMENT

To explore the effect of PRMT5 on MYC-driven HCC development, spontaneous HCC was induced using TetO-MYC/LAP-tTA transgenic mice by withdrawal of doxycycline to turn on the MYC transgene (MYC-ON) and initiate liver tumorigenesis. Administration of GSK3326595, an oral PRMT5 inhibitor in clinical trials for non-Hodgkin lymphoma and solid tumor treatment,[16] to MYC-ON mice for 12 weeks after MYC activation decreased tumor incidence, multiplicity, liver weight, and serum alanine aminotransferase (ALT) and aspartate aminotransferase (AST) levels compared with vehicle-treated mice (Fig. 3A,B; Supporting Table S3). All vehicle-treated MYC-ON mice versus 37.5% of the GSK3326595-treated MYC-ON mice developed liver tumors. GSK3326595-treated MYC-OFF mice, which did not express MYC transgene nor develop tumors, exhibited similar liver weight and serum ALT and AST levels as vehicle-treated MYC-OFF mice (Fig. 3B), indicating no obvious liver toxicity under normal conditions. Moreover, a short-term 2-week administration of GSK3326595 to MYC-ON mice after the MYC transgene was activated for 8 weeks decreased tumor multiplicity, liver weights, and serum ALT and AST levels compared with vehicle-treated mice (Fig. 3C,D; Supporting Table S4). To monitor tumor progression in one mouse over time, serial MRI scans were performed. Although liver tumors continued to grow after administration of GSK3326595, the growth rate was significantly lower than vehicle-treated tumors (Fig. 3E).

Both mRNA and protein levels of MYC and PRMT5 were induced in liver tumors compared with adjacent nontumor tissues, which were also observed after short-term and long-term GSK3326595 treatment (Fig. 4A,B; Supporting Fig. S3A,B). Instead, GSK3326595 treatment inhibited PRMT5 activity, as revealed by decreased protein levels of its two products, H3R8me2s and H4R3me2s, in both liver tumors and adjacent nontumor tissues (Fig. 4A). Parallel to repressed PRMT5 activity, the levels of SDMA, but not ADMA, were decreased in both GSK3326595-treated liver tumors and adjacent nontumor tissues as compared with vehicle-treated mice (Fig. 4C,D). Similarly, serum and urinary levels of SDMA, but not ADMA, were reduced in GSK3326595-treated MYC-ON mice compared with those of vehicle-treated mice (Fig. 4E,F; Supporting Fig. S3C,D). Collectively, these data indicate that blocking PRMT5 activity in liver by GSK3326595 suppresses MYC-induced liver tumorigenesis.

INHIBITION OF PRMT5 SUPP RESSES CELL PROLIFERAT ION THROUGH UP-REGULAT ION OF p27

PRMT5 was reported to play roles in cell proliferation, cell death, migration, and invasion.[17] The PRMT5 inhibitor GSK3326595 may exert antiproliferative and antineoplastic properties. Indeed, GSK3326595 treatment suppressed cell proliferation in liver as indicated by Ki-67 staining (Supporting Fig. S4A,B) and decreased colony formation in MYC-overexpressing JHH-7 cells (Supporting Fig. S4C). To investigate the downstream events after PRMT5 inhibition, RNA sequencing (RNA-seq) was performed on JHH-7 cells infected with short hairpin PRMT5 lentivirus. KEGG enrichment revealed that the top

pathways affected were associated with cell proliferation, and Gene Ontology (GO) enrichment showed that the top pathways affected were related to cell cycle pathways (Supporting Fig. S5A-C). Most differential genes enriched in TNF and advanced glycation end products (AGEs) and its receptor RAGE (receptor for AGE) pathway were covered by MAPK signaling pathway (Supporting Fig. S5C). Studies reported that PRMT5 interacted with MAPK, NF-κB, and E2F signaling pathways, known for their roles in controlling cell fate and tumorigenesis, by direct histone or posttranslational methylation or indirect ways in different cell types, but little is known in HCC cells.[18–20] Therefore, phosphorylation of MAPKs (extracellular signal-regulated kinase [ERK], c-Jun N-terminal kinase [JNK], and p38) and p65 (NF-κB) proteins as well as the mRNA expression of NF-κB–dependent cytokine genes and *E2F* genes were examined in JHH-7 cells. PRMT5 ablation increased both phospho-JNK (p-JNK) and p-p38, whereas PRMT5 overexpression decreased their phosphorylation. PRMT5 did not markedly alter the phosphorylation status of ERK and p65 (Supporting Fig. S5D). At the mRNA level, PRMT5 overexpression suppressed transcription, whereas PRMT5 knockdown or inhibition conversely elevated transcription of NF-κB target genes and *E2F7* in HCC cells (Supporting Fig. S5E,F).

To further explore the downstream targets for the MYC-PRMT5 axis, the mRNA expression of several tumor suppressor genes was examined in nontumor tissues from GSK3326595-treated MYC-ON mice (Fig. 5A). Among the mRNAs examined, GSK3326595 treatment up-regulated *Cdkn1b* (*p27*) mRNA in liver, and a similar induction of p27 protein levels was observed (Fig. 4A). Consistent with these data, *p27* mRNA was also increased in livers from DEN-treated $Myc^{\Delta Hep,ERT2}$ mice compared with DEN-treated $Myc^{fl/fl}$ mice (Fig. 5B). Furthermore, the levels of p27 mRNA and protein were decreased in liver tumors compared with adjacent nontumor tissues from patients with HCC and negatively correlated with the expression of MYC, PRMT5, and its two products, H3R8me2s and H4R3me2s (Fig. 5C; Supporting Fig. S2A-E). Similar results were also obtained from a published 159 paired HCC tumor and adjacent liver dataset,[21] which showed that *PRMT5* mRNA was up-regulated, whereas *p27* mRNA down-regulate in tumors compared with adjacent livers, and a negative correlation was observed in the adjacent livers (Supporting Fig. S6A). These findings suggest that PRMT5 drives HCC tumorigenesis through inhibition of p27.

p27 is a tumor suppressor that has the ability to block cancer cell proliferation and induce cell cycle arrest.[22] In different HCC cell lines, GSK3326595 repressed cell proliferation, as revealed by cell viability and colony formation assays (Fig. 5D; Supporting Fig. S6B,C) along with induced p27 expression (Fig. 5E). Silencing of PRMT5 increased p27 expression and attenuated cell proliferation and colony formation, whereas overexpression of PRMT5 decreased p27 expression and enhanced cell proliferation and colony formation in JHH-7 cells (Fig. 5D,E; Supporting Fig. S6D). Flow cytometry analysis showed that PRMT5 inhibition induced cell cycle arrest in G2/M phase and could even induce cell cycle arrest in S phase, whereas PRMT5 overexpression exhibited the opposite effect (Supporting Fig. S6E,F). In addition, overexpression of PRMT5 decreased, whereas inhibition of PRMT5 by CMP5 increased *p27* mRNA expression in HepG2 cells (Supporting Fig. S6G). To test whether PRMT5 directly methylates the H3R8 residue or the H4R3 residue around the *p27* promoter region, ChIP assays were performed in JHH-7 cells. Silencing of PRMT5 decreased the enrichment of both H3R8me2s and H4R3me2s on the *p27* promoter,

supporting the view that *p27* was a methylation target of PRMT5 (Fig. 5F). These results demonstrate that PRMT5 negatively regulates p27 transcription, which then promotes cancer cell proliferation.

GSK3326595 PROMOTES LYMPHOCYTE INFILTRATION IN LIVER TUMORS

To further explore the mechanisms underlying repressed HCC development by GSK3326595 treatment, RNA-seq analysis was carried out with RNAs from GSK3326595-treated MYC-ON mice. When comparing GSK3326595-treated tumors with vehicle-treated tumors, 144 mRNAs were significantly increased and 98 mRNAs were significantly decreased (Fig. 6A,B). Surprisingly, pathway enrichment analysis revealed that the top KEGG pathways affected by GSK3326595 treatment in liver tumors were related to immunity (Fig. 6C). Among the top 10 up-regulated mRNAs, the transcripts of 3 components of the MHC II molecule family, *H2-Ab1*, *H2-Aa*, and *Cd74* and the MHC II transactivator *Ciita* (class II major histocompatibility complex transactivator), were increased by more than 10-fold in GSK3326595-treated liver tumors versus vehicle-treated liver tumors, which was confirmed by direct quantification (Fig. 6D). Immunofluorescence staining revealed a similar induction of CD74 and MHC II (Fig. 6E). Lymphocyte infiltration was induced in GSK3326595-treated liver tumors as indicated by CD45.1, CD4, and CD8 staining (Fig. 6E,F). These observations suggest a potential role for PRMT5 in tumor immunity associated with HCC.

To clarify whether increased MHC II expression and lymphocyte infiltration is the reason for or a phenomenon secondary to attenuated tumor growth, MYC-ON mice after activation of the MYC transgene for 8 weeks were treated with GSK3326595 for 3 days. At this point, there was no significant difference in tumor number, liver weight, and serum ALT and AST levels between vehicle-treated and GSK3326595-treated mice (Fig. 7A,B). However, the total infiltrating $CD45.1^+$ leukocytes in liver tumors were increased by GSK3326595 treatment (Fig. 7C). An expansion of natural killer (NK) cells, $CD4^+$ T cells, $CD8^+$ T cells, dendritic cells (DC), and monocytes was observed in GSK3326595-treated liver tumors, whereas no changes were noted in other immune subsets including B ells, natural killer T (NKT) cells, and granulocytic-myeloid–derived suppressor cell (Fig. 7C). The mean fluorescence intensities of MHC II on tumor-infiltrating $CD45.1^+$ leukocytes and DC cells were both significantly increased by GSK3326595 treatment (Fig. 7D). The expression of CD74 and MHC II only partially merged with CD45.1 (Fig. 6E), suggesting that nonleukocytes, perhaps liver tumor cells themselves, also expressed CD74 and MHC II. Despite the constitutive expression pattern of MHC II on professional antigen-presenting cells, many other cell types, including tumor cells, can express MHC II. Tumor-specific MHC II expression may increase recognition of a tumor by the immune system and therefore may play an important role in immunotherapy.[23] To examine the regulation of MHC II and related pathway components by PRMT5 in nonleukocytes of liver tumors, primary hepatocytes and the JHH-7 cells were treated with GSK3326595. As expected, GSK3326595 significantly up-regulated the mRNA levels of MHC II–related genes in both cells (Fig. 7E). To test whether PRMT5 directly methylates MHC II–related genes (*CIITA* and *CD74*), ChIP assays were performed in JHH-7 cells. Silencing of PRMT5 decreased the enrichment of H3R8me2s and H4R3me2s on both the *CIITA* and *CD74* promoters (Fig. 7F), supporting that PRMT5 directly regulates MHC II expression by histone methylation.

Together, these data revealed that inhibition of PRMT5 induced MHC II expression in both leukocytes and hepatocytes and thus enforced immune cell infiltration into liver tumors, which may contribute to an enhanced antitumor immune response and repressed tumor growth.

To determine whether the tumor suppressive function of GSK3326595 is dependent on T cells, α-CD3, α-CD4, and α-CD8 antibodies were administered to MYC-ON mice to deplete T cells, $CD4^+$ T cells, and $CD8^+$ T cells (Supporting Fig. S7), respectively. When compared with the adjacent nontumor tissues, *MYC* and *Prmt5* mRNAs were up-regulated in liver tumors to similar levels in both vehicle-treated and GSK3326595-treated MYC-ON mice with T-cell depletion (Supporting Fig. S8A,B). GSK3326595 treatment decreased levels of H4R3me2s in both the liver tumors and adjacent nontumor tissues, regardless of the presence of T cells (Supporting Fig. S8C). In T cell–depleted and $CD8^+$ T cell–depleted mice, PRMT5 inhibition tended to decrease tumor multiplicity, liver weights, and serum ALT and AST levels (Supporting Fig. S8D-G, L-O). In $CD4^+$ T cell–depleted mice, serum ALT and AST levels were significantly lower in the GSK3326595-treated group, whereas tumor number and liver weight tended to decrease (Supporting Fig. S8H-K). Collectively, these data showed that the antitumor effect of PRMT5 inhibition was largely weakened by T-cell depletion, but GSK3326595 still had some ability to decrease tumorigenesis, even in the T cell–depleted mice. Note that p27 expression was still increased in the nontumor tissues of GSK3326595-treated T cell–depleted mice (Supporting Fig. S8C), suggesting that PRMT5 inhibition of MYC-driven tumor growth depends on both intrinsic immune response and the p27 pathway.

PRMT5 INHIBITION SYNERGIZES WITH Anti–PD-1 IMMUNE CHECKPOINT THERAPY IN HCC

To further determine whether PRMT5 inhibition could improve the efficacy of immune checkpoint therapy (ICT) in HCC, the combination of GSK3326595 and anti–PD-1 treatment in MYC-ON mice and two types of HCC cell line–derived xenograft models were investigated. When combined with anti–PD-1 treatment in MYC-transgenic mice, GSK3326595 at 50 mg/kg/day significantly suppressed tumor growth compared with anti–PD-1 monotherapy (Fig. 8A). However, combination therapy did not show any additional suppression compared with the GSK3326595 treatment at the same dose alone due to the potent antitumor efficacy of GSK3326595. Therefore, the dose of GSK3326595 was reduced to 25 mg/kg/day. When combined with anti–PD-1 antibody, GSK3326595 at lower dose did show better therapeutic efficacy in HCC tumorigenesis compared with either treatment alone.

H22 and Hepa1–6 HCC xenograft models were next subjected to the combined therapy. Compared with monotherapy, the combination of GSK3326595 and anti–PD-1 antibody augmented the antitumor response in both models (Fig. 8B,C). To determine whether the difference in tumor growth was associated with T cells, the lymphocytes in tumors were profiled at the endpoint. Compared with the vehicle+IgG group, the combined therapy remarkably induced the infiltration of total T cells, $CD4^+$ T cells, and $CD8^+$ T cells in both xenograft models, whereas either GSK3326595 or anti–PD-1 monotherapy only

slightly increased the infiltration (Fig. 8D). Collectively, these results demonstrated that the combination of PRMT5 inhibitor and anti–PD-1 treatment showed superior antitumor response than either treatment alone.

Discussion

Aberrant high levels of MYC expression are broadly present in cancers, including HCC. Herein, an MYC-dependent change in PRMT5 expression and its product SDMA was uncovered in HCC. MYC modulates PRMT5 expression by direct transcriptional activation, paralleled by elevated SDMA levels in the urine. This MYC-PRMT5–based regulatory circuit is essential for HCC development, as PRMT5 inhibition impedes tumorigenesis in a transgenic mouse model of MYC-driven HCC. Mechanistically, inhibition of PRMT5 increases tumor suppressor p27 expression through release of H4R3me2s-mediated and H3R8me2s-mediated transcriptional repression and thus suppresses cell proliferation. Moreover, PRMT5 inhibition promotes MHC II expression and immune cell infiltration in liver tumors, potentially enhancing the antitumor immune response. Together, these findings unveil PRMT5 as an epigenetic executer of MYC for its repressive transcriptional regulation of the downstream genes, thus highlighting inhibition of PRMT5 as a promising strategy for MYC-driven HCC treatment (Fig. 8E).

Abnormal metabolism has been considered an important characteristic of tumors, and comprehensive metabolism studies could help clarify the pathogenesis and provide potential targets for treatments. Although studies have been performed exploring the metabolic changes associated with HCC,[24] to date, there have been few studies exploring MYC-related changes in the metabolome associated with HCC, despite the key role of MYC in liver tumorigenesis. In the current study, urine samples from saline-treated and DEN-treated $Myc^{fl/fl}$ and $Myc^{\Delta Hep,ERT2}$ mice were subjected to metabolomic analysis. Several methylation-related metabolites including 1-methylnicotinamide, DMA, and 5-methylcytidine were among the top down-regulate metabolites in DEN-treated $Myc^{\Delta Hep,ERT2}$ mice, suggesting that MYC might affect epigenetic modifications, which is one of the key events during HCC progression.[25] Aberrant arginine methylation is implicated in the development of multiple cancers and reported to influence various biological processes such as signal transduction, chromatin remodeling, and proliferation.[26] Therefore, the current study focused on the change of DMA and clarified the molecular mechanism underlying the elevation of this tumor-related metabolite.

There are two types of DMA: ADMA catalyzed by type I protein N-arginine methyltransferases (PRMT1/2/3/6/8 and coactivator-associated arginine methyltransferase [CARM]1) and SDMA by type II protein arginine methyltransferases (PRMT5/9). Urinary SDMA, but not ADMA, was found increased in HCC and decreased by hepatic *Myc* disruption, likely due to induced PRMT5 expression by MYC in liver tumors. The relationship between MYC and PRMT5 has been studied in some other cancers. MYC recruits PRMT5 to form a complex that modulates MYC binding and histone methylation at target promoters in glioblastoma and gastric cancer.[27,28]

PRMT5 posttranslationally regulates MYC stability in medulloblastoma and pancreatic cancer.[29,30] PRMT5 represses tumor suppressor miRNAs that down-regulate MYC in lymphoma.[31] MYC also directly up-regulates PRMT5 transcription and thus safeguards proper pre-mRNA splicing in lymphomagenesis.[32] The current work demonstrates that PRMT5 is encoded by an MYC target gene, suggesting that MYC drives repressive transcription at least partially through PRMT5 in HCC. Consistent with the mouse data, the mRNA and protein level as well as activity of PRMT5 were induced in liver tumors compared with adjacent nontumor tissues from patients with HCC, along with elevated SDMA in the urine.

PRMT5 is amplified in several human malignancies, including liver cancer, lymphoma, and glioblastoma, and high levels of PRMT5 are generally associated with poor prognosis.[33] PRMT5 is postulated to regulate various biological processes such as cell death, proliferation, migration, invasion, DNA repair, and mRNA splicing at transcriptional or posttranscriptional levels through arginine methylation of histone or nonhistone substrates, respectively.[11,17,32,34] Some studies have shown that loss of PRMT5 exerts antiproliferative and antineoplastic functions both *in vitro* and *in vivo*.[11,32,35] Because of the profound role of PRMT5 in tumorigenesis, therapy against PRMT5 is considered a promising strategy for cancer treatment. Over the past few years, many PRMT5 inhibitors were discovered, including *S*-adenosyl methionine (SAM) uncompetitive inhibitors like EPZ015666, SAM competitive inhibitors like DS-437 and N-alkyl-9H-carbozole analogs like CMP5.[36] To date, none of the PRMT5 inhibitors have been approved by FDA for therapeutic use. EPZ015938, which was licensed to GSK (GSK3326595), is an improved compound derived from EPZ015666 and has entered phase I clinical trials for solid tumors and non-Hodgkin lymphoma (NCT02783300).[16] Although most PRMT5 inhibitors were preclinically tested on cell lines or xenograft models, few studies have explored their efficacy in the treatment of autochthonous primary HCC. In the present work, GSK3326595 dramatically reduced the tumor burden in transgenic MYC-driven HCC in mice. In agreement with the well-documented role of PRMT5 in promoting cell proliferation, PRMT5 knockdown or inhibition by GSK3326595 significantly suppressed HCC cell proliferation and induced cell cycle arrest by activation of p27, JNK, p38 MAPK, and E2F7 signaling pathways.

Other than suppressed cell proliferation, RNA-seq analysis suggested that MHC II expression was induced and immunity-related pathways were enriched by PRMT5 inhibition. Short-term GSK3326595 treatment without changes in tumor burden revealed that increased leukocyte infiltration and enhanced MHC II expression were initial events to suppressed tumorigenesis, suggesting an unexpected immune cell recruiting and antigen-presenting enhancing role of GSK3326595 in HCC. Thus, in addition to the MYC-PRMT5-p27regulatory axis in hepatocytes, GSK3326595 may also impair HCC development through promoting antitumor immune response. However, the mechanisms underlying GSK3326595-regulated immune response are unclear. Data from T-cell depletion experiments suggested that GSK3326595 repressed HCC development partially dependent on T cells. There are two possible explanations for this dependence: (1) GSK3326595 directly affects T cell function and thus suppresses HCC; (2) GSK3326595 affects the function of tumor cells or other non-T cells, which recruit T cells as effector cells, resulting in suppression of HCC. The HCC microenvironment consists of various cell types including

tumor cells, immune cells, and other stromal cells like endothelial cells.[12] Different cells function together as a complexed network. PRMT5 is essentially expressed in almost all cell types and implicated in multiple cell functions.[37,38] Direct or indirect effect of GSK3326595 on nonparenchymal cells other than hepatocytes or tumor cells cannot be excluded in this case. Detailed mechanisms of PRMT5 inhibition on HCC development still await further study.

Previous studies investigating the role of PRMT5 in HCC seldom, if ever, focused on tumor immunity, which is an important aspect of HCC progression and treatment. The growth of HCC is facilitated by diminished antitumor immune response. Multiple immunosuppressive mechanisms in HCC have been proposed, including defective antigen presentation, recruitment of immunosuppressive myeloid and lymphoid cell populations, impaired NK and T-cell functions, and up-regulation of immune checkpoint pathways.[12–14] So far, immune checkpoint inhibitors against cytotoxic T lymphocyte antigen 4 (CTLA-4), PD-1, and its ligand programmed death ligand 1 (PD-L1) are the most developed molecules used to boost antitumor immunity and have changed the landscape of cancer therapy, including HCC.[39] Combinatorial use of immunotherapy with other treatments is also a popular option.[14] A recent study characterized a tumor-intrinsic function of PRMT5 in promoting immunosuppression by controlling cyclic guanosine monophosphate-adenosine monophosphatesynthase (cGAS)/stimulator of interferon genes (STING) and NOD-, LRR-and CARD-containing 5 (NLRC5) pathways in melanoma and identified that combination of PRMT5 inhibition with ICT limited the growth of murine melanoma tumors and enhanced therapeutic efficacy compared with the effect of either treatment alone.[40] The current study showed that inhibition of PRMT5 by GSK3326595, in addition to its antiproliferative function, induced immune cell infiltration into liver tumors and promoted antigen presentation through up-regulation of MHC II molecules. The genes for the MHC II transactivator CIITA and component of MHC II molecule CD74 were identified as direct targets of PRMT5. A combination of GSK3326595 with anti–PD-1 therapy limited growth of MYC-driven spontaneous HCC and murine xenograft liver tumors (H22 and Hepa1–6) and enhanced therapeutic efficacy compared with the effect of either treatment alone, suggesting that PRMT5 inhibition could synergize with ICT-like anti–PD-1 treatment to treat HCC.

In conclusion, the present work unravels an MYC-dependent induction of SDMA in HCC with increased expression of *PRMT5* as an MYC target gene. Inhibition of PRMT5 by GSK3326595 ameliorates MYC-driven HCC development through both suppressed proliferation through up-regulation of p27 and enhanced antitumor immunity through induction of immune cell infiltration and MHC II expression in liver tumors. Therefore, these findings delineate the functional importance of MYC-PRMT5 axis in HCC tumorigenesis, argue for the potential application of PRMT5 inhibitors as a therapeutic strategy for MYC-driven HCC, and also provide a rationale to apply combination of PRMT5 inhibition and ICT in “immune-cold” tumors.

Supplementary Material

Refer to Web version on PubMed Central for supplementary material.

Acknowledgment:

We thank Tim F. Greten from National Cancer Institute (NCI) for providing the LAP-tTA and TetO-MYC transgenic mice. We thank Martin Lizak from National Institutes of Health (NIH) Mouse Imaging Facility for help with the MRI scanning of the mouse liver. We thank Jingmin Shi, Xiaoxia Gao, and Dasheng Lu for help with animal dissection and sample collection.

Supported by the National Cancer Institute Intramural Research Program, the National Natural Science Foundation of China (91957116), the Shanghai Rising-Star Program (20QA1411200), and the Research Fund of State Key Laboratory of Drug Research (SIMM2004KF-04 and SIMM2003ZZ-02).

Abbreviations:

ADMA	asymmetric dimethylarginine
ALT	alanine aminotransferase
AST	aspartate aminotransferase
CARM	coactivator-associated arginine methyltransferase
CIITA	class II major histocompatibility complex transactivator
ChIP	chromatin immunoprecipitation
Ciita	class II major histocompatibility complex transactivator
DC	dendritic cell
DEN	diethylnitrosamine
DMA	dimethylarginine
ICT	immune checkpoint therapy
JNK	c-Jun N-terminal kinase
KEGG	Kyoto Encyclopedia of Genes and Genomes
MAX	protein max
MHC II	major histocompatibility complex class II
MYC	myelocytomatosis
MYC-OFF	myelocytomatosis transgene turned off
MYC-ON	myelocytomatosis transgene turned on
NK	natural killer
PD-1	programmed cell death protein 1
PRMT	protein arginine N-methyltransferase
RNA-seq	RNA sequencing

SDMA	symmetric dimethylarginine

REFERENCES

1). Sung H, Ferlay J, Siegel RL, Laversanne M, Soerjomataram I, Jemal A, et al. Global cancer statistics 2020: GLOBOCAN estimates of incidence and mortality worldwide for 36 cancers in 185 countries. CA Cancer J Clin 2021. 10.3322/caac.21660. [Epub ahead of print]

2). Kudo M, Finn RS, Qin S, Han KH, Ikeda K, Piscaglia F, et al. Lenvatinib versus sorafenib in first-line treatment of patients with unresectable hepatocellular carcinoma: a randomised phase 3 non-inferiority trial. Lancet 2018;391:1163–1173. [PubMed: 29433850]

3). Meyer N, Penn LZ. Reflecting on 25 years with MYC. Nat Rev Cancer 2008;8:976–990. [PubMed: 19029958]

4). Shachaf CM, Kopelman AM, Arvanitis C, Karlsson A, Beer S, Mandl S, et al. MYC inactivation uncovers pluripotent differentiation and tumour dormancy in hepatocellular cancer. Nature 2004;431:1112–1117. [PubMed: 15475948]

5). Qu A, Jiang C, Cai Y, Kim JH, Tanaka N, Ward JM, et al. Role of Myc in hepatocellular proliferation and hepatocarcinogenesis.J Hepatol 2014;60:331–338. [PubMed: 24096051]

6). Kaposi-Novak P, Libbrecht L, Woo HG, Lee YH, Sears NC, Conner EA, et al. Central role of c-Myc during malignant conversion in human hepatocarcinogenesis. Cancer Res 2009;69:2775–2782. [PubMed: 19276364]

7). Grandori C, Cowley SM, James LP, Eisenman RN. The Myc/Max/Mad network and the transcriptional control of cell behavior. Annu Rev Cell Dev Biol 2000;16:653–699. [PubMed: 11031250]

8). Herman JG, Baylin SB. Gene silencing in cancer in association with promoter hypermethylation. N Engl J Med 2003;349:2042–2054. [PubMed: 14627790]

9). Zheng BN, Ding CH, Chen SJ, Zhu K, Shao J, Feng J, et al. Targeting PRMT5 activity inhibits the malignancy of hepatocellular carcinoma by promoting the transcription of HNF4alpha. Theranostics 2019;9:2606–2617. [PubMed: 31131056]

10). Shimizu D, Kanda M, Sugimoto H, Shibata M, Tanaka H, Takami H, et al. The protein arginine methyltransferase 5 promotes malignant phenotype of hepatocellular carcinoma cells and is associated with adverse patient outcomes after curative hepatectomy. Int J Oncol 2017;50:381–386. [PubMed: 28101581]

11). Li Z, Zhang J, Liu X, Li S, Wang Q, Di Chen, et al. The LINC01138 drives malignancies via activating arginine methyltransferase 5 in hepatocellular carcinoma. Nat Commun 2018;9:1572. [PubMed: 29679004]

12). Sia D, Jiao Y, Martinez-Quetglas I, Kuchuk O, Villacorta-Martin C, Castro de Moura M, et al. Identification of an immune-specific class of hepatocellular carcinoma, based on molecular features. Gastroenterology 2017;153:812–826. [PubMed: 28624577]

13). Prieto J, Melero I, Sangro B. Immunological landscape and immunotherapy of hepatocellular carcinoma. Nat Rev Gastroenterol Hepatol 2015;12:681–700. [PubMed: 26484443]

14). Hato T, Goyal L, Greten TF, Duda DG, Zhu AX. Immune checkpoint blockade in hepatocellular carcinoma: current progress and future directions. HEPATOLOGY 2014;60:1776–1782. [PubMed: 24912948]

15). Ma C, Han M, Heinrich B, Fu Q, Zhang Q, Sandhu M, et al. Gut microbiome-mediated bile acid metabolism regulates liver cancer via NKT cells. Science 2018;360:eaan5931. [PubMed: 29798856]

16). Rasco D, Tolcher A, Siu LL, Heinhuis K, Postel-Vinay S, Barbash O, et al. Abstract CT038: a phase I, open-label, dose-escalation study to investigate the safety, pharmacokinetics, pharmacodynamics, and clinical activity of GSK3326595 in subjects with solid tumors and non-Hodgkin's lymphoma. Can Res 2017;77:CT038.

17). Stopa N, Krebs JE, Shechter D. The PRMT5 arginine methyltransferase: many roles in development, cancer and beyond. Cell Mol Life Sci 2015;72:2041–2059. [PubMed: 25662273]

18). Kanade SR, Eckert RL. Protein arginine methyltransferase 5 (PRMT5) signaling suppresses protein kinase Cdelta- and p38delta-dependent signaling and keratinocyte differentiation. J Biol Chem 2012;287:7313–7323. [PubMed: 22199349]

19). Cho EC, Zheng S, Munro S, Liu G, Carr SM, Moehlenbrink J, et al. Arginine methylation controls growth regulation by E2F-1. EMBO J 2012;31:1785–1797. [PubMed: 22327218]

20). Wei H, Wang B, Miyagi M, She Y, Gopalan B, Huang DB, et al. PRMT5 dimethylates R30 of the p65 subunit to activate NF-kappaB. Proc Natl Acad Sci U S A 2013;110:13516–13521. [PubMed: 23904475]

21). Gao Q, Zhu H, Dong L, Shi W, Chen R, Song Z, et al. Integrated proteogenomic characterization of HBV-related hepatocellular carcinoma. Cell 2019;179:561–577.e522. [PubMed: 31585088]

22). Serres MP, Zlotek-Zlotkiewicz E, Concha C, Gurian-West M, Daburon V, Roberts JM, et al. Cytoplasmic p27 is oncogenic and cooperates with Ras both in vivo and *in vitro*. Oncogene 2011;30:2846–2858. [PubMed: 21317921]

23). Axelrod ML, Cook RS, Johnson DB, Balko JM. Biological consequences of MHC-II expression by tumor cells in cancer. Clin Cancer Res 2019;25:2392–2402. [PubMed: 30463850]

24). Wang X, Zhang A, Sun H. Power of metabolomics in diagnosis and biomarker discovery of hepatocellular carcinoma. HEPATOLOGY 2013;57:2072–2077. [PubMed: 23150189]

25). Nishida N, Goel A. Genetic and epigenetic signatures in human hepatocellular carcinoma: a systematic review. Curr Genomics 2011;12:130–137. [PubMed: 21966251]

26). Yang Y, Bedford MT. Protein arginine methyltransferases and cancer. Nat Rev Cancer 2013;13:37–50. [PubMed: 23235912]

27). liu M, Yao B, Gui t, Guo C, Wu X, Li J, et al. PRMT5-dependent transcriptional repression of c-Myc target genes promotes gastric cancer progression. Theranostics 2020;10:4437–4452. [PubMed: 32292506]

28). Favia A, Salvatori L, Nanni S, Iwamoto-Stohl LK, Valente S, Mai A, et al. The protein arginine methyltransferases 1 and 5 affect Myc properties in glioblastoma stem cells. Sci Rep 2019;9:15925. [PubMed: 31685892]

29). Chaturvedi NK, Mahapatra S, Kesherwani V, Kling MJ, Shukla M, Ray S, et al. Role of protein arginine methyltransferase 5 in group 3 (MYC-driven) medulloblastoma. BMC Cancer 2019;19:1056. [PubMed: 31694585]

30). Qin YI, Hu Q, Xu J, Ji S, Dai W, Liu W, et al. PRMT5 enhances tumorigenicity and glycolysis in pancreatic cancer via the FBW7/cMyc axis. Cell Commun Signal 2019;17:30. [PubMed: 30922330]

31). Karkhanis V, alinari l, Ozer HG, Chung J, Zhang X, Sif S, et al. Protein arginine methyltransferase 5 represses tumor suppressor miRNAs that down-regulate CYCLIN D1 and c-MYC expression in aggressive B-cell lymphoma. J Biol Chem 2020;295:1165–1180. [PubMed: 31822509]

32). Koh CM, Bezzi M, Low DHP, Ang WX, Teo SX, Gay FPH, et al. MYC regulates the core pre-mRNA splicing machinery as an essential step in lymphomagenesis. Nature 2015;523:96–100. [PubMed: 25970242]

33). Kim H, Ronai ZA. PRMT5 function and targeting in cancer. Cell Stress 2020;4:199–215. [PubMed: 32743345]

34). Tamiya H, Kim H, Klymenko O, Kim H, Feng Y, Zhang T, et al. SHARPIN-mediated regulation of protein arginine methyltransferase 5 controls melanoma growth. J Clin Invest 2018;128:517–530. [PubMed: 29227283]

35). Jin Y, Zhou J, Xu F, Jin B, Cui L, Wang Y, et al. Targeting methyltransferase PRMT5 eliminates leukemia stem cells in chronic myelogenous leukemia. J Clin Invest 2016;126:3961–3980. [PubMed: 27643437]

36). Richters A Targeting protein arginine methyltransferase 5 in disease. Future Med Chem 2017;9:2081–2098. [PubMed: 29076773]

37). Inoue M, Okamoto K, Terashima A, Nitta T, Muro R, Negishi-Koga T, et al. Arginine methylation controls the strength of γc-family cytokine signaling in T cell maintenance. Nat Immunol 2018;19:1265–1276. [PubMed: 30323341]

38). Litzler LC, Zahn A, Meli AP, Hébert S, Patenaude AM, Methot SP, et al. PRMT5 is essential for B cell development and germinal center dynamics. Nat Commun 2019;10:22. [PubMed: 30604754]

39). Topalian SL, Hodi FS, Brahmer JR, Gettinger SN, Smith DC, McDermott DF, et al. Safety, activity, and immune correlates of anti-PD-1 antibody in cancer. N Engl J Med 2012;366:2443–2454. [PubMed: 22658127]

40). Kim H, Kim H, Feng Y, Li Y, Tamiya H, Tocci S, et al. PRMT5 control of cGAS/STING and NLRC5 pathways defines melanoma response to antitumor immunity. Sci Transl Med 2020;12:eaaz5683. [PubMed: 32641491]

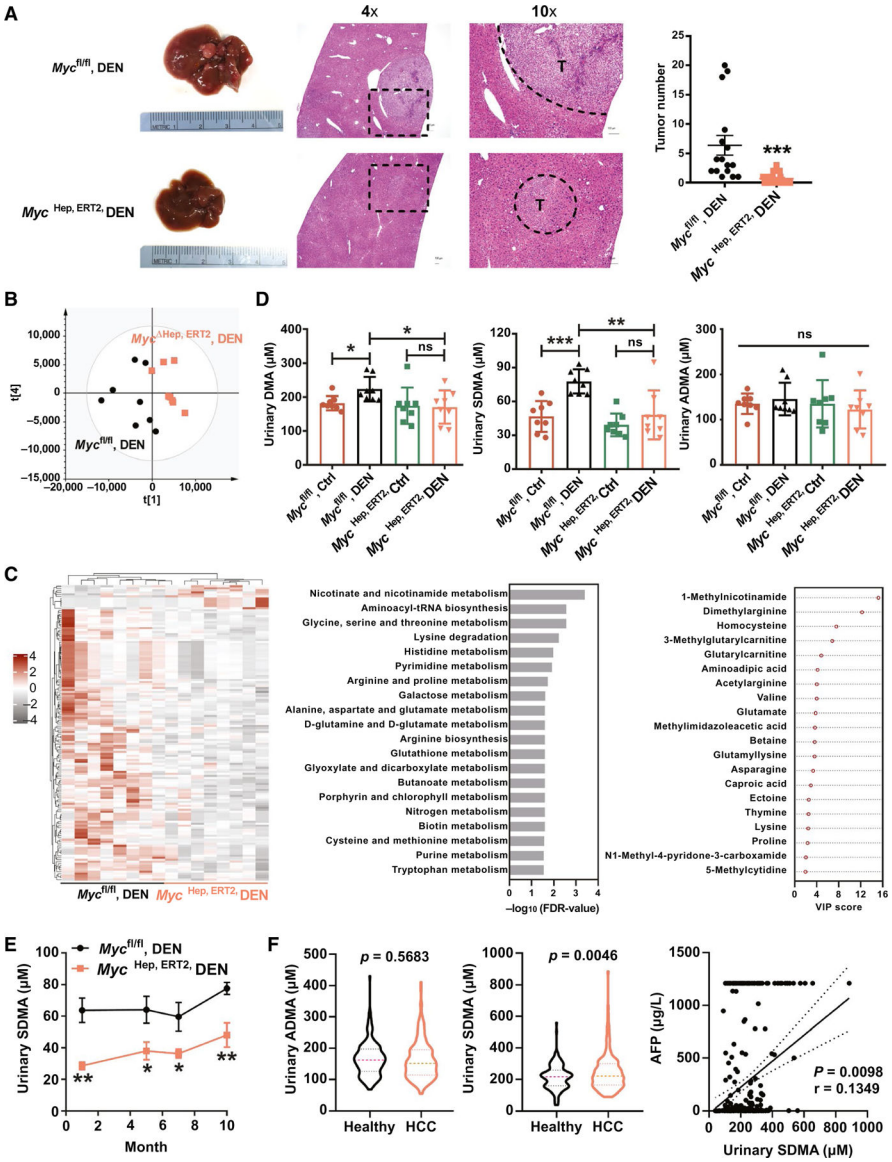

FIG. 1.

Urinary SDMA is MYC-dependently increased in HCC. (A) Representative liver images and hematoxylin and eosin staining of liver sections from DEN-treated *Myc*$^{fl/fl}$ and *Myc*$^{\Delta Hep,ERT2}$ mice (left) and quantification of surface tumor number (right). Scale bar, 100 μm. n = 16–23/group. (B) Partial least squares discriminant analysis (PLS-DA) analysis of the creatinine-normalized urinary metabolites from DEN-treated *Myc*$^{fl/fl}$ and *Myc*$^{\Delta Hep,ERT2}$ mice. n = 8/group. (C) Heat map of the differential metabolites (variable importance in projection [VIP] score >1; *P* value < 0.05) (left). The top 20 KEGG pathway enrichments (middle). VIP scores of top 20 identified metabolites from PLS-DA (right). (D) Quantitation of DMA, SDMA, and ADMA in urine. n = 8/group. (E) Time course of SDMA in urine. n = 8/group. (F) Quantitation of ADMA and SDMA in the urine from patients with HCC (n = 196) and healthy controls (n = 176) and correlation of serum alpha-fetoprotein (AFP) with

urinary SDMA assessed by nonparametric Spearman's test. *$P < 0.05$, **$P < 0.01$, ***$P < 0.001$. Abbreviations: FDR, false discovery rate; ns, not significant; tRNA, transfer RNA.

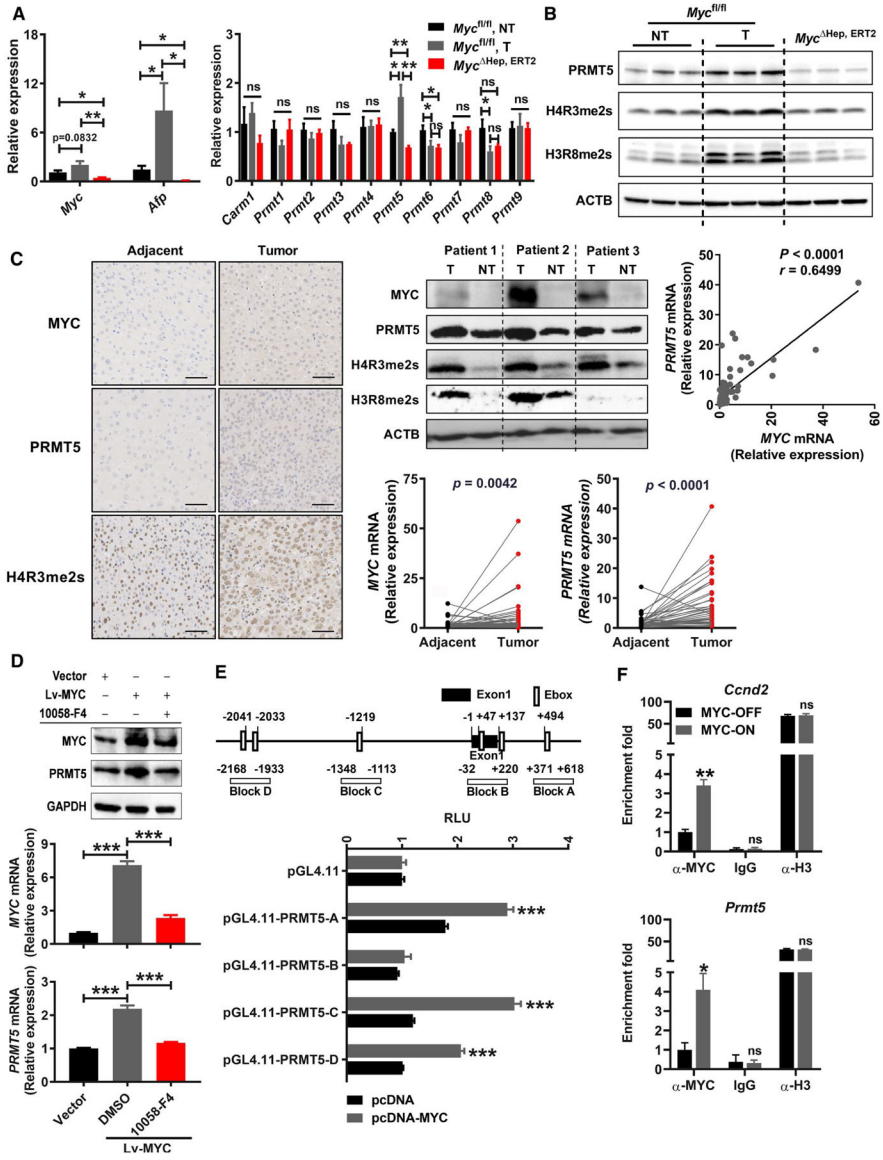

FIG. 2.

MYC directly regulates *PRMT5* transcription in HCC. (A) The mRNA levels of *Myc* and alpha-fetoprotein (*Afp*) and protein arginine methyltransferase genes in the liver tumors (T) and nontumors (NT) from DEN-treated $Myc^{fl/fl}$ and $Myc^{\Delta Hep,ERT2}$ mice. n = 6–8/group. (B) Representative immunoblots of indicated proteins in the liver tumors (T) and nontumors (NT) from DEN-treated $Myc^{fl/fl}$ and $Myc^{\Delta Hep,ERT2}$ mice. (C) Representative IHC staining of MYC, PRMT5, and H4R3me2s on HCC tumor and adjacent liver sections (scale bar, 50 μm, left), representative immunoblots of indicated proteins in paired human HCC tumor (T) and adjacent nontumor tissues (NT) (middle, top), *MYC* and *PRMT5* mRNA expression in paired tumors and adjacent nontumor tissues from patients with HCC (n = 40) (middle, bottom), and correlation of *MYC* and *PRMT5* mRNA expression in liver tumors from patients with HCC assessed by nonparametric Spearman's test (right, top). (D) MYC and PRMT5 protein levels (top) and *MYC* and *PRMT5* mRNA levels (bottom) in JHH-7 cells

infected with lentiviral control (Vector) or MYC expression lentivirus (Lv-MYC) and treated with MYC inhibitor 10058-F4. n = 3/group. (E) A schematic diagram of the human *PRMT5* promoter (−3 kb) illustrating the E-boxes in the regulatory region and the fragments used for luciferase reporter assay. *PRMT5* promoter activity was assessed by luciferase reporter assay. n = 4/group. (F) ChIP assays of cyclin D2 [*Ccnd2*] (positive control, top) and *Prmt5* (bottom) on the liver tissues from MYC-ON and MYC-OFF mice. n = 3/group. $*P < 0.05$, $**P < 0.01$, $***P < 0.001$. Abbreviations: ACTB, β-actin; Carm, coactivator-associated arginine methyltransferase; GAPDH, glyceraldehyde 3-phosphate dehydrogenase, Lv, lentivirus, ns, not significant.

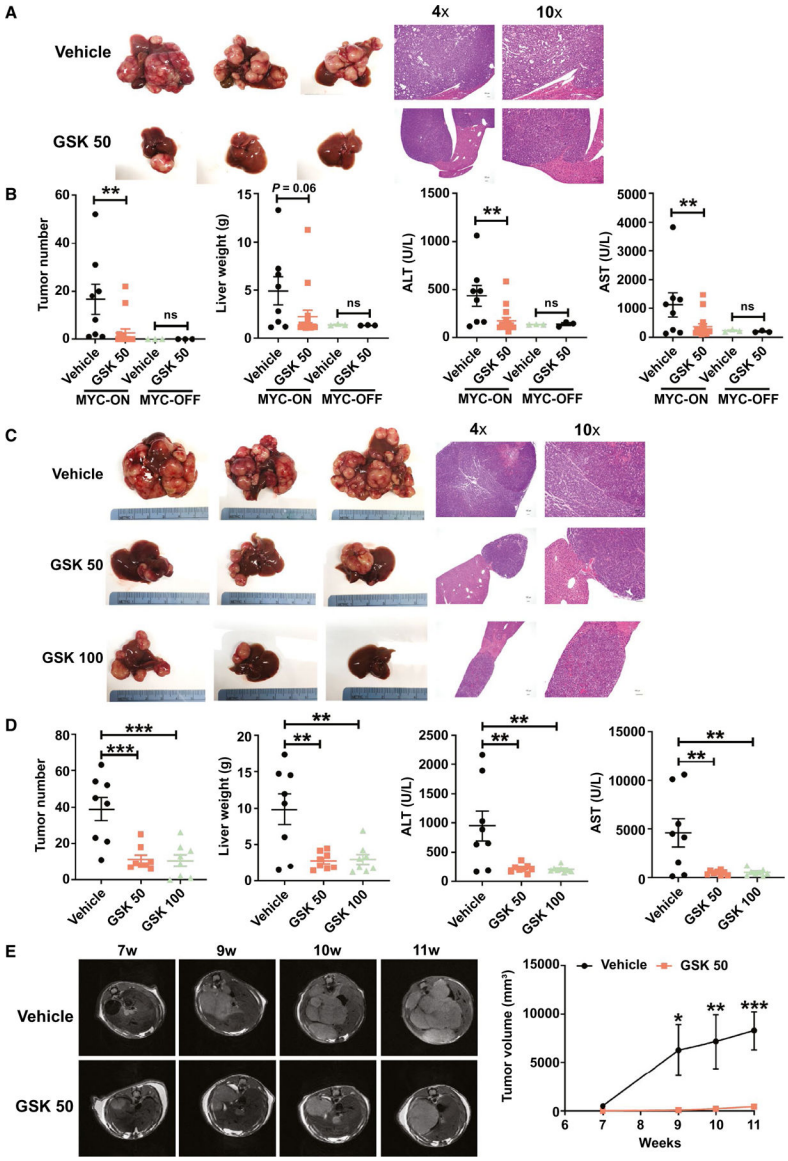

FIG. 3.

PRMT5 inhibition attenuates MYC-driven HCC development in mice. (A) Representative liver images and hematoxylin and eosin (H&E) staining of liver sections. Scale bar, 100 μm. (B) Surface tumor number, liver weight, serum ALT and AST levels. (A,B) MYC-ON mice and MYC-OFF mice were treated with vehicle or 50 mg/kg GSK3326595 (GSK 50) for 12 weeks. n = 3–16/group. (C) Representative liver images and H&E staining of liver sections. Scale bar, 100 μm. (D) Surface tumor number, liver weight, serum ALT and AST levels. (C,D) MYC-ON mice were treated with vehicle or 50 mg/kg GSK3326595 (GSK 50) or 100 mg/kg GSK3326595 (GSK 100) for 2 weeks after the MYC transgene was activated for 8 weeks. n = 8/group. (E) MYC-ON mice were treated with vehicle or 50 mg/kg GSK3326595 (GSK 50) for 4 weeks after the MYC transgene was activated for 7 weeks. n = 4–6/group. Representative MRI images of livers (left) and liver tumor volume (right). *$P < 0.05$, **$P < 0.01$, ***$P < 0.001$. Abbreviation: ns, not significant.

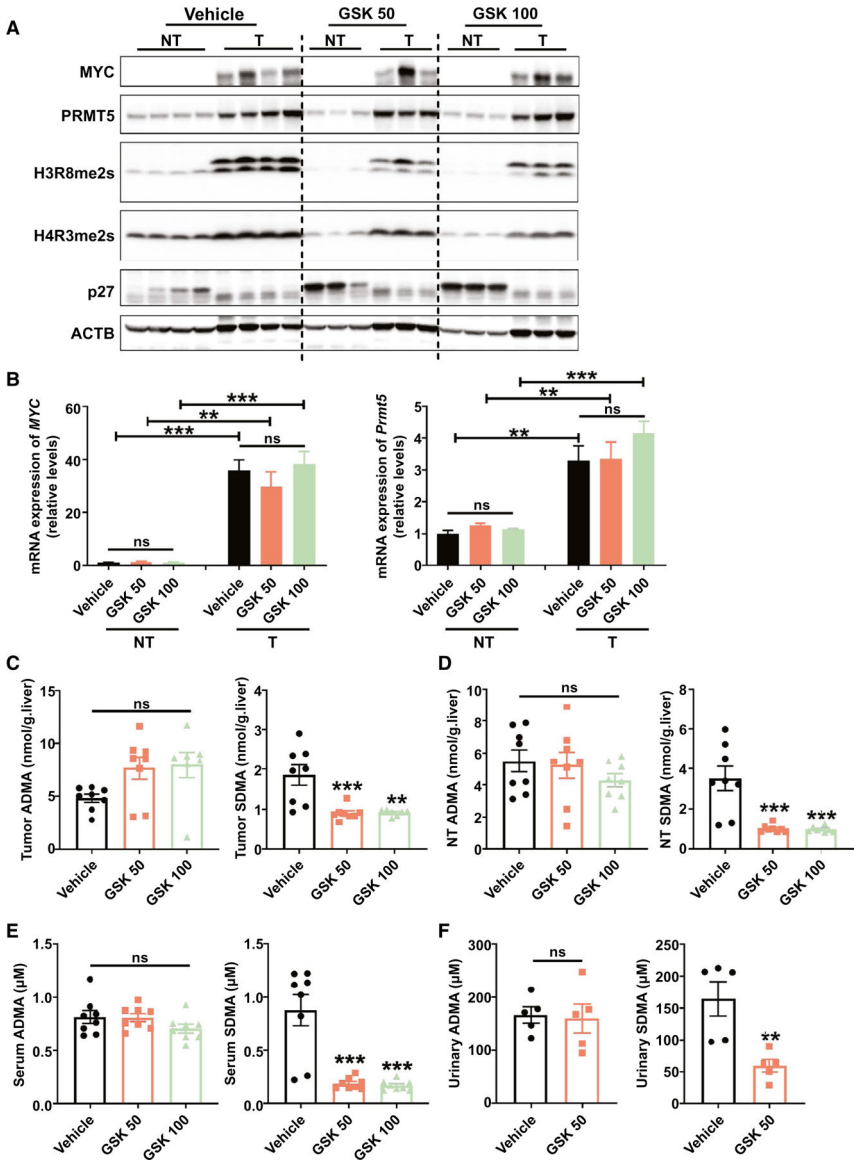

FIG. 4.

GSK3326595 represses MYC-induced PRMT5 activity and decreases SDMA levels in mice. MYC-ON mice were treated with vehicle or 50 mg/kg GSK3326595 (GSK 50) or 100 mg/kg GSK3326595 (GSK 100) for 2 weeks after the MYC transgene was activated for 8 weeks. (A) Representative immunoblots of indicated proteins in the liver tumors (T) and adjacent nontumor tissues (NT). (B) *MYC* and *Prmt5* mRNA expression in the liver tumors (T) and adjacent nontumor tissues (NT). n = 7–8/group. (C) ADMA and SDMA levels in liver tumors. n = 7–8/group. (D) ADMA and SDMA levels in nontumor tissues. n = 8/group. (E) Serum ADMA and ADMA levels. n = 8/group. (F) Urinary ADMA and SDMA levels. n = 5/group. $^{**}P < 0.01$, $^{***}P < 0.001$. Abbreviations: ACTB, β-actin; ns, not significant.

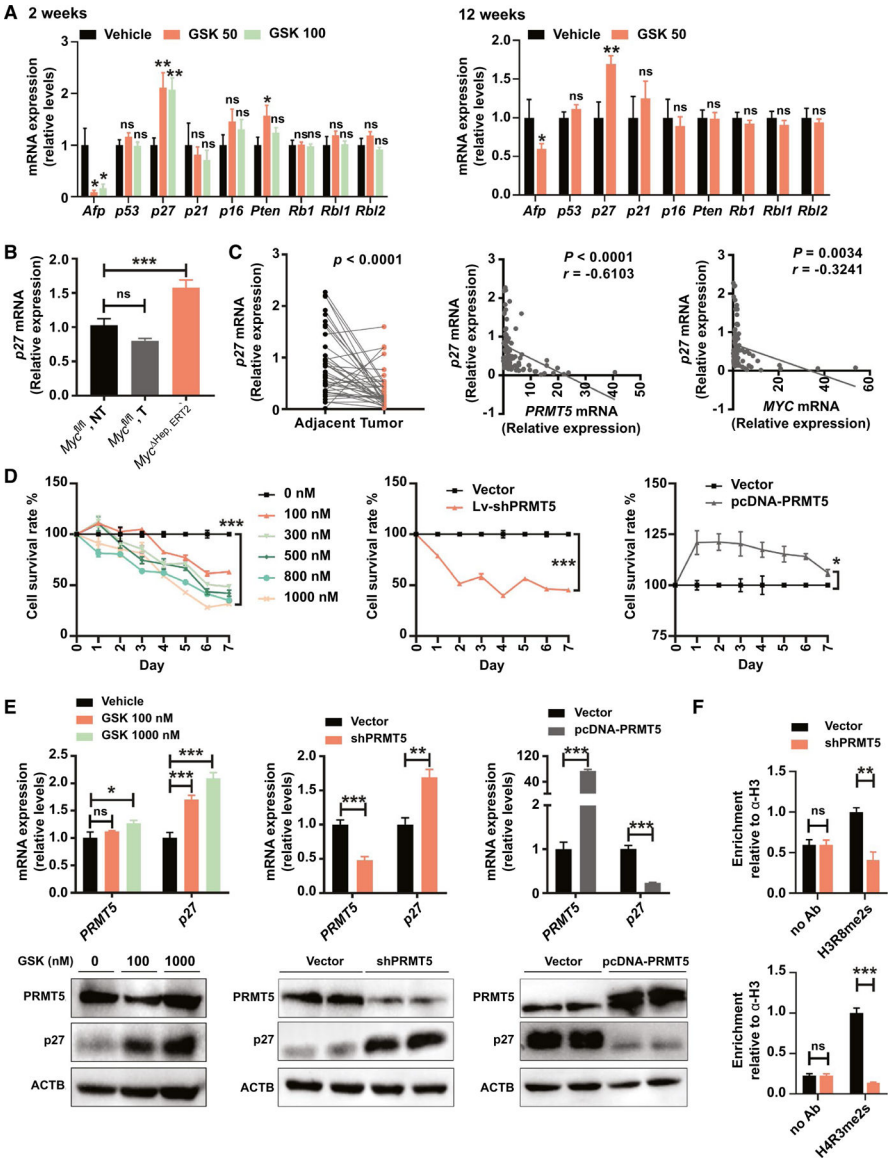

FIG. 5.

PRMT5 promotes cell proliferation by methylating tumor suppressor p27. (A) mRNA expression of alpha-fetoprotein (*Afp*) and tumor suppressor genes in hepatic nontumor tissues of MYC-ON mice treated with vehicle or 50 mg/kg GSK3326595 (GSK 50) or 100 mg/kg GSK3326595 (GSK 100) for 2 weeks after the MYC transgene was activated for 8 weeks (left) and MYC-ON mice treated with vehicle or GSK 50 for 12 weeks after activation of the MYC transgene (right). n = 7–16/group. (B) *p27* mRNA expression in the liver tumors (T) or nontumors (NT) from DEN-treated $Myc^{fl/fl}$ and $Myc^{\Delta Hep,ERT2}$ mice. n = 6–8/group. (C) *P27* mRNA expression (left) and its correlation with *PRMT5* (middle) and *MYC* (right) in paired tumors and adjacent nontumor tissues from patients with HCC assessed by nonparametric Spearman's test. n = 40. (D) Cell proliferation of JHH-7 cells treated with GSK3326595 at indicated concentrations (n = 3/group, left), infected with lentiviral control or short hairpin (sh) PRMT5 (n = 6/group, middle), or transfected

with empty vector or pcDNA-PRMT5 overexpression construct (n = 3/group, right). (E) mRNA and protein levels of PRMT5 and p27 in JHH-7 cells treated with 100 or 1,000 nM GSK3326595 for 24 h (n = 3/group for mRNA, left), or infected with lentiviral control or shPRMT5 (n = 3/group for mRNA, middle), or transfected with empty vector or pcDNA-PRMT5 overexpression construct (n = 3/group for mRNA, right). (F) ChIP assay of *p27* on JHH-7 cells infected with lentiviral control or shPRMT5. n = 3/group. *$P < 0.05$, **$P < 0.01$, ***$P < 0.001$. Abbreviations: α-H3, anti-histone H3; Ab, antibody; ACTB, β-actin; Lv, lentivirus; ns, not significant; Pten, phosphatase and tensin homolog; Rb, retinoblastoma protein; Rbl, retinoblastoma-like protein.

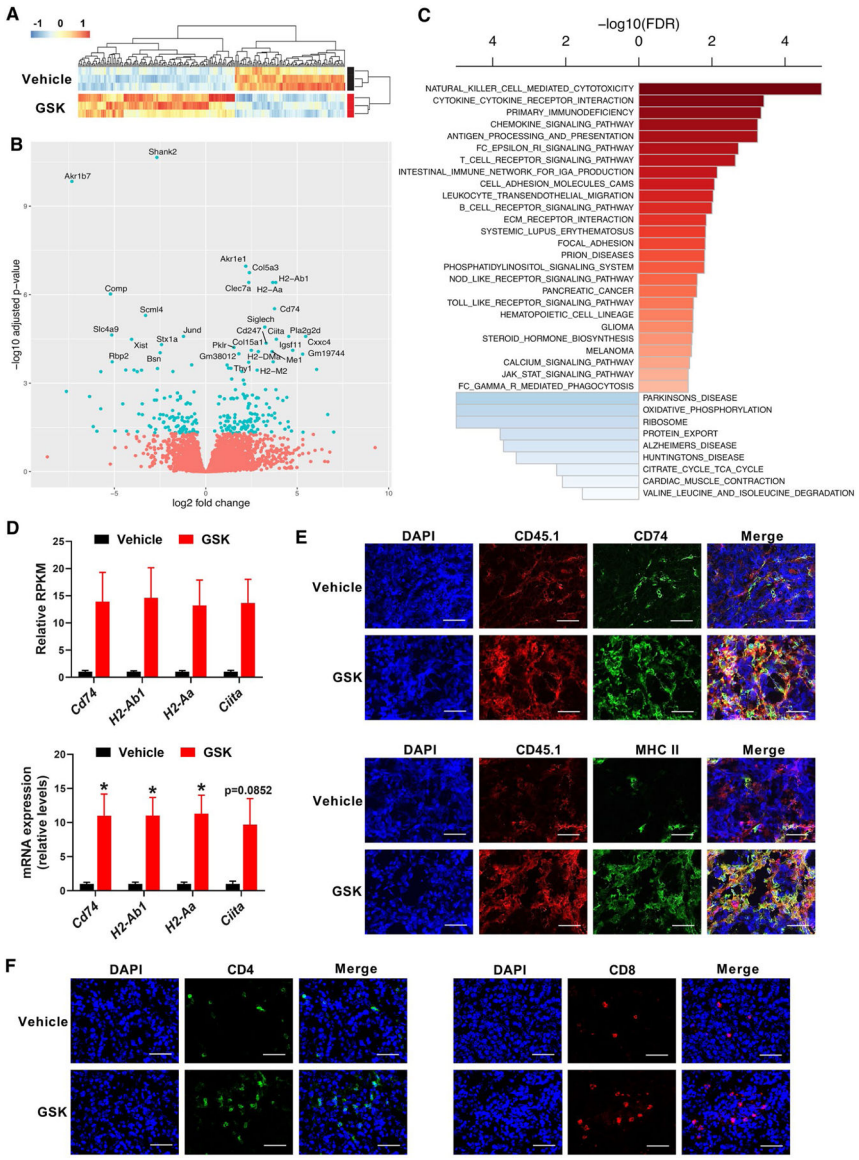

FIG. 6.

PRMT5 inhibition boosts lymphocyte infiltration in MYC-driven HCC. MYC-ON mice were treated with vehicle or 50 mg/kg GSK3326595 for 2 weeks after the MYC transgene was activated for 8 weeks. (A) Heatmap of the differentially expressed genes (fold change >1.5, adjusted *P* value (*P-adj*) < 0.05). (B) Volcano plot. The blue dots represent the differential expressed genes (*P-adj* < 0.05). The top 30 significant genes were labeled. (C) The top KEGG pathway enrichments (false discovery rate [FDR] < 0.05). The red highlighted up-regulated pathways, and blue highlighted down-regulated pathways. (D) Relative reads per kilobase million (RPKM; top) and mRNA levels (bottom) of MHC II–related genes in the liver tumors. n = 3/group. (E) Representative immunofluorescence staining of CD45.1, CD74, and MHC II in the liver tumors. Scale bar, 50 μm. (F) Representative immunofluorescence staining of CD4 and CD8 in the liver tumors. Scale bar, 50 μm. **P* < 0.05. Abbreviations: Akr, aldo-keto reductase; Bsn, bassoon; CAMS,

cell adhesion molecules; Clec7a, C-type lectin domain family 7, member a; Col5a3, collagen, type V, alpha 3; Comp, cartilage oligomeric matrix protein; Cxxc, CpG-binding protein; ECM, extracellular matrix; FC EPISILON RI, a cell-surface receptor for the constant fragment region of immunoglobulin E molecules; IGA, Immunoglobulin A; Igsf, immunoglobulin superfamily; JAK, Janus kinase; Jund, jun D proto-oncogene; NOD, nucleotide-binding oligomerization domain; Pklr, pyruvate kinase liver and red blood cell; Pla2g2d, phospholipase A2, group IID; Rbp, retinol binding protein; Scml, scm polycomb group protein like; Shank2, SH3 and multiple ankyrin repeat domains 2; Slc, solute carrier family; STAT, signal transducer and activator of transcription; Stx, Shiga toxin; TCA, trichloroacetic acid; Thy, thymus cell antigen.

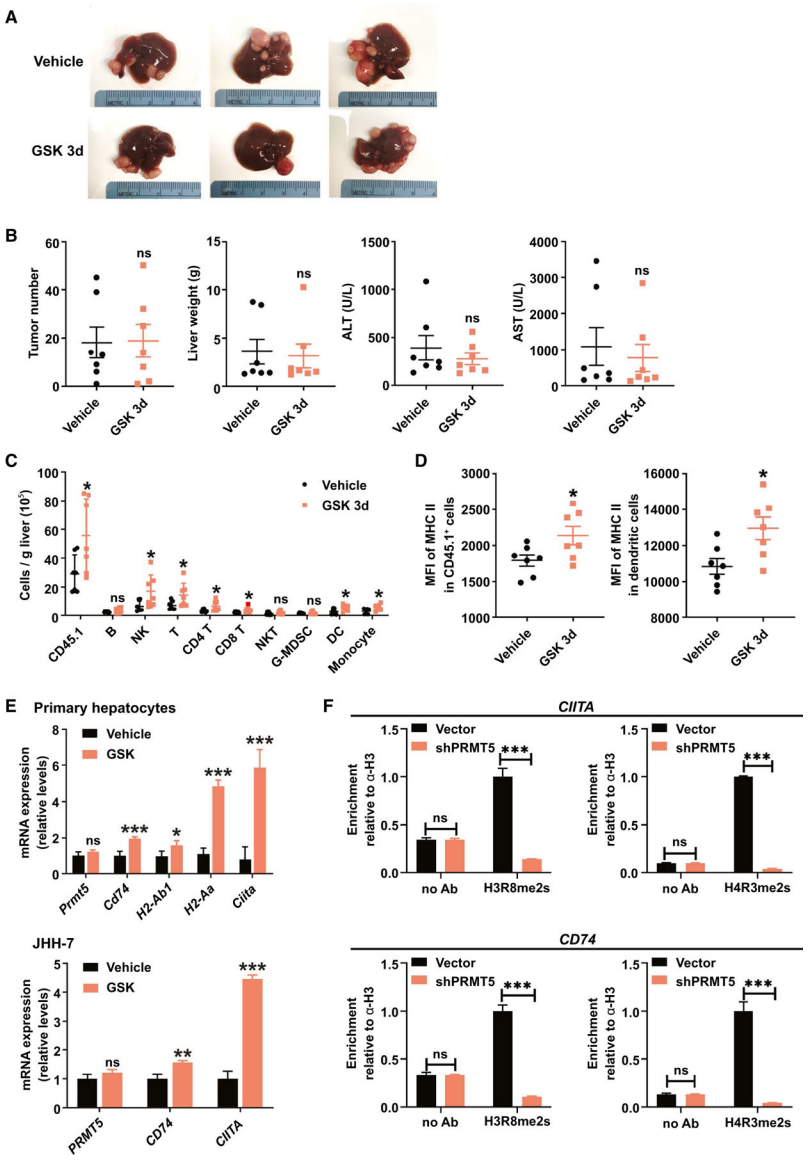

FIG. 7.

PRMT5 inhibition initiates lymphocyte infiltration in MYC-driven HCC at an early stage. (A) Representative liver images. (B) Surface tumor number, liver weight, serum ALT and AST levels. (C) Liver tumor-infiltrating immune cells. (D) Mean fluorescence intensity of MHC II in CD45.1^{+} leukocytes and dendritic cells (DCs). (A-D) MYC-ON mice were treated with vehicle or 50 mg/kg GSK3326595 for 3 days after the MYC transgene was activated for 8 weeks. n = 7/group. (E) mRNA expression of *Prmt5*/PRMT5 and MHC II–related genes in primary hepatocytes (top) and JHH-7 cells (bottom) treated with 300 nM GSK3326595. n = 3/group. (F) ChIP assays of MHC II–related genes on JHH-7 cells infected with lentiviral control or short hairpin (sh) PRMT5. n = 3/group. *$P < 0.05$, **$P < 0.01$, ***$P < 0.001$. Abbreviations: α-H3, anti-histone H3; Ab, antibody; B, B lymphocyte; DC, dendritic cell; G-MDSC, granulocytic-myeloid-derived suppressor cell;

MFI, mean fluorescence intensity; NKT, neutral killer T lymphocyte; ns, not significant; T, T lymphocyte.

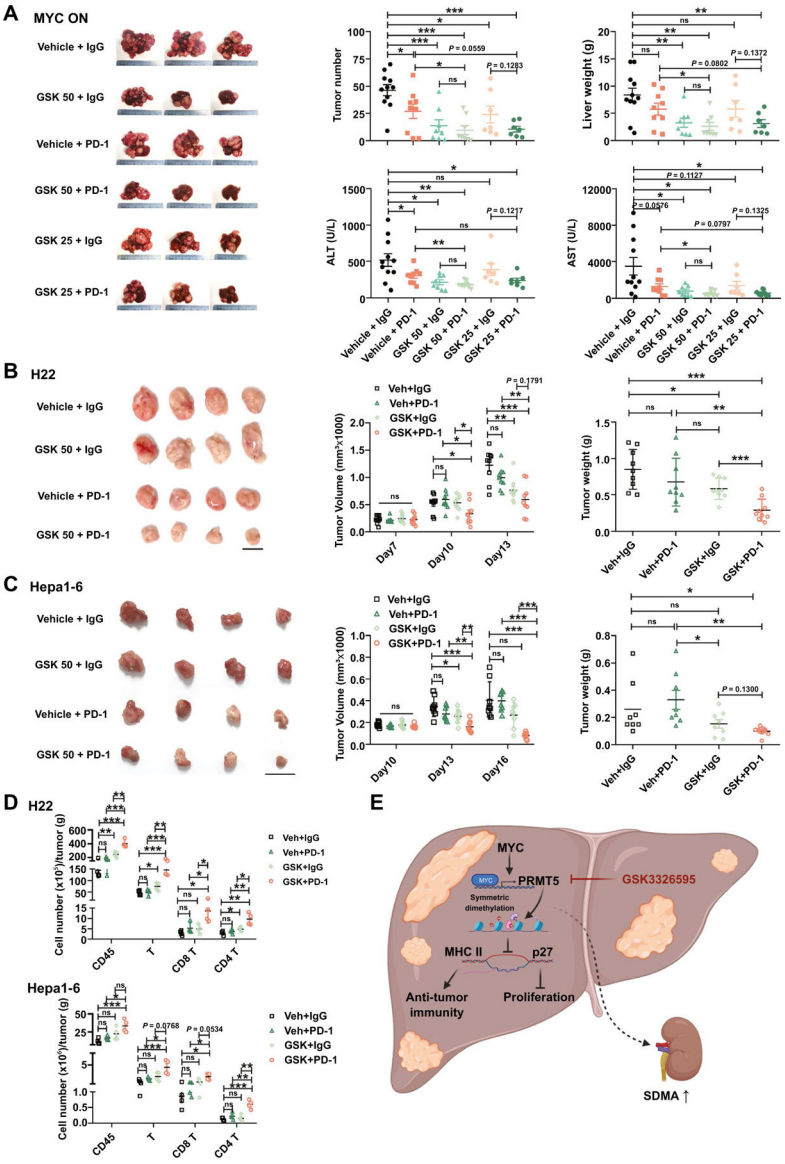

FIG. 8.

PRMT5 inhibition enhances the efficacy of anti–PD-1 ICT in HCC. (A) Representative liver images, surface tumor number, liver weight, serum ALT and AST levels. MYC-ON mice were orally administered vehicle or 25 or 50 mg/kg GSK3326595 (GSK 25 and GSK 50) daily combined with intraperitoneal injection of 200 μg IgG or anti–PD-1 antibody every 3 days for 2 weeks after the MYC transgene was activated for 8 weeks. (B) Representative tumor images (scale bar, 1 cm, left), tumor volume (middle), and tumor weight (right) of Hepa1–6 xenografts. n = 8. (C) Representative tumor images (scale bar, 1 cm, left), tumor volume (middle), and tumor weight (right) of H22 xenografts. n = 9. (D) Tumor-infiltrating immune cells for H22 (top) and Hepa1–6 (bottom) xenografts. n = 4. (B-D) Hepa1–6 and H22 cells were grafted into C57BL/6J mice, which were subsequently treated with vehicle or 50 mg/kg/day GSK3326595 daily combined with intraperitoneal injection of 200 μg IgG or anti–PD-1 antibody every 3 days for a week. (E) A schematic diagram

depicting the MYC-PRMT5 regulatory axis in HCC. MYC induces PRMT5 expression in HCC, paralleled by increased SDMA levels in the serum and urine. Inhibition of PRMT5 with GSK3326595 increases p27 expression, thus suppressing cell proliferation. Moreover, PRMT5 inhibition promotes MHC II expression and immune cell infiltration in liver tumors, potentially enhancing antitumor immune response. Both pathways contribute to impeded HCC development. *$P < 0.05$, **$P < 0.01$, ***$P < 0.001$. Abbreviations: ns, not significant; Veh, vehicle.